

although the external field was varied between 0–10 000 Oe and the frequency between 5 to 40 Mc/sec. No explanation was suggested. It might perhaps be possible to observe the effect of H_i on the quadrupole resonance of Cl ^{35,37} at these low temperatures. Nevertheless, it would be interesting to undertake careful experiments particularly in the region 1–4°K on NQR and Zeeman effect. As the asymmetry parameter is large, all the four Zeeman components corresponding to the tran-

sition $(\pm\frac{3}{2}) \rightarrow (+-)$ may be observed even in zero field.

ACKNOWLEDGMENTS

The authors are deeply indebted to Professor K. R. Rao for his guidance and kind interest throughout the progress of work. Our grateful thanks are also due to Dr. C. R. K. Murty and Dr. D. Premaswarup for helpful discussions.

Paramagnetic Susceptibility of Metallic Lithium and Sodium by Electron Spin Resonance Saturation*

RICHARD HECHT†

IBM Watson Laboratory, Columbia University, New York, New York

(Received 12 June 1963)

The total conduction electron spin moment of lithium and sodium dispersions has been measured in polarizing fields of about 10 G. The steady-state change in sample polarization at electron spin resonance was detected and then extrapolated to the limit of full saturation. Surprisingly, it was found that because the rf fields were linearly polarized and comparable to the polarizing field, the saturation level did not increase monotonically with rf field strength. The data were in good fit with saturation curves derived by means of numerical integration of the modified Bloch equation. The conduction electron spin susceptibility χ_s for lithium at 300°K was $(1.96 \pm 0.10) \times 10^{-6}$ cgs volume units. The relative values of χ_s in lithium were the same at 300, 77, and 1.5°K, within an estimated uncertainty of 3%, and the relative values of χ_s in sodium were the same at 77 and 1.5°K, within an estimated uncertainty of 5%.

I. INTRODUCTION

DIRECT measurements of conduction electron spin susceptibility χ_s were first made by Schumacher and Slichter¹ on lithium and sodium at 77°K. Their method was later refined by Schumacher and Vehse,² who extended the measurements on sodium to 4.2°K. As expected, the values found for χ_s were higher than those predicted by Pauli³ in the free-electron approximation, because the exchange interaction favors spin alignment. The best agreement is with the values of χ_s calculated by Bohm and Pines,⁴ and by Shimizu.⁵

In addition to permitting a comparison with theory, knowledge of χ_s is useful in estimating the interaction between conduction electrons and nuclear spins. In particular, the average probability density P_F of Fermi level electrons at the nuclear site can be inferred from the Knight shift,⁶ which is proportional to the product

$P_F \chi_s$. Moreover, knowledge of χ_s permits a surer test of the Korringa relation⁷ connecting χ_s , the Knight shift, the electronic specific heat, and that part of the nuclear relaxation rate associated with the contact hyperfine field. For these reasons, it seemed worthwhile to repeat the measurements of χ_s by a different method.

In the present experiment, a transverse linearly polarized rf field at electron spin resonance is applied to a longitudinally polarized sample, and the resulting change in longitudinal electron spin moment is detected. Only the average, steady-state response is observed. The change in moment is proportional to the degree of saturation Z , defined by $Z = 1 - \langle M_z \rangle / \chi_s H_0$, where H_0 is the polarizing field strength, and $\langle M_z \rangle$ is the longitudinal spin magnetization at resonance. The original electron spin moment is inferred by extrapolating the detected signal to the limit $Z = 1$. To do this, the data must be fitted to the computed dependence of Z on rf field strength, based on the modified Bloch equation.⁸ These computations are essential, for we find that Z does not increase monotonically with the rf field strength, but shows broad local maxima owing to the fact that the rf field is linearly polarized and comparable to H_0 .

* Based on a thesis submitted in partial fulfillment of the requirements for the degree of Doctor of Philosophy at Columbia University.

† Present address: RCA Laboratories, Princeton, New Jersey.
¹ R. T. Schumacher and C. P. Slichter, Phys. Rev. **101**, 58 (1957).

² R. T. Schumacher and W. E. Vehse, J. Phys. Chem. Solids **24**, 297, (1963).

³ W. Pauli, Ann. Physik **41**, 81 (1927).

⁴ D. Pines, in *Solid State Physics* edited by F. Seitz and D. Turnbull (Academic Press Inc., New York, 1956), Vol. I, p. 367.

⁵ Masao Shimizu, J. Phys. Soc. Japan **15**, 2220 (1960).

⁶ W. D. Knight, in *Solid State Physics*, edited by F. Seitz and

D. Turnbull, (Academic Press Inc., New York, 1956), Vol. II, p. 105.

⁷ J. Korringa, Physica **16**, 601 (1950).

⁸ R. K. Wangsness, Phys. Rev. **98**, 927 (1955).

Looked at in another way, in these measurements the change in longitudinal spin moment is used to detect the degree of saturation Z . Another quantity resulting from electron spin saturation, and again proportional to Z , is Overhauser enhancement of nuclear spin polarization.⁹ In a second paper,¹⁰ a measurement of Overhauser enhancement in lithium and sodium is reported. The plots of Overhauser enhancement against rf field strength are in good fit both with the theoretical saturation curves derived from the modified Bloch equation and with the plots of change in electron spin moment against rf field strength. Since the separate results of the two measurements confirm quite unrelated theoretical predictions, the credibility of each result is strengthened.

II. EXPERIMENTAL PROCEDURE

Detection Scheme

Figure 1 is a simplified block diagram of the electronic apparatus used for room temperature measurements of χ_s in lithium. For the measurements of the temperature dependence of χ_s in lithium and sodium, it was found necessary to substitute a shorted coaxial line for the rf hairpin. This resulted in a larger filling factor and in relief from the annoyances of rf discharges in helium vapor and of paramagnetic background from exposed portions of the cryostat. Functionally, however, the shorted coaxial line was identical to the rf hairpin.

The samples, metallic dispersions in wax or mineral oil, were polarized in a steady field H_0 of about 10 G. Simultaneously, a 28-Mc/sec linearly polarized, transverse rf field was applied in square bursts at a 280 cps repetition rate. Rf duty cycles of about 3% were used when saturating the spin system; duty cycles of up to 50% were used for low rf intensity line-shape measurements. The rf level was monitored by a direct flux link to the rf field.

A standard phase-sensitive detection procedure was followed. The sample magnetic moment along H_0 was smaller during an rf burst than in the interval between bursts. This alternating moment induced a 280 cps emf in the pickup coil surrounding the cryostat tail; the coil output was then filtered, amplified, and sent to the lock-in detector. To calibrate, the rf was cut off and a reference solenoid of known dimensions was substituted for the sample. An alternating current of the same waveform and phase as the rf envelope was fed to the solenoid. Because this waveform was quite square, and because the electron spin-lattice relaxation time is short ($T_1 \approx 10^{-7}$ sec), the solenoid magnetization truly simulated the sample magnetization. Corrections were made for filling factor differences and for solenoid shrinkage at low temperature.

⁹ A. W. Overhauser, Phys. Rev. **92**, 411 (1953).

¹⁰ R. Hecht and A. G. Redfield, following paper, Phys. Rev. **132**, 972 (1963).

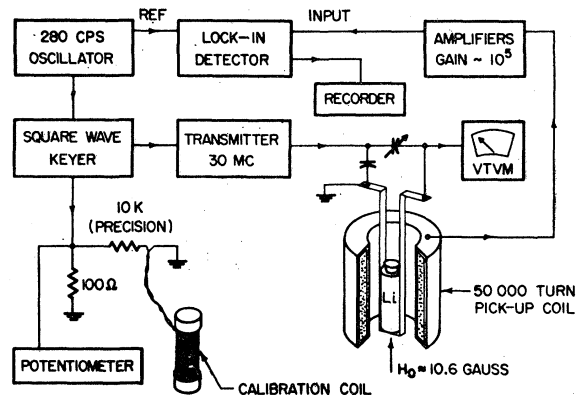


FIG. 1. Block diagram of the experimental arrangement. Not shown are the Helmholtz coils or the cryostat tail which surrounds the rf hairpin.

Measurements

Preliminary to saturation measurements, the resonance line shape was plotted by varying H_0 , keeping the rf level fixed at some low intensity. The line centers were found for both directions of current through the Helmholtz coils, and the linewidth was measured so that the theoretical approach to saturation could be computed. Since it was H_0 rather than the frequency which was varied, corrections were made for the displacement of the resonance peaks from the true line centers. Corrections were also made for slight saturation broadening; this was preferable to operating at such low rf intensities that accuracy was sacrificed. The estimated uncertainty in line center is less than 1%.

Saturation measurements were then made at the same radio frequency, and at a number of different rf intensities. H_0 was set first at one and then at the other line center, and the average of the two signals was taken. This procedure prevented mistaking for signal any 280-cps background which was independent of the sign of H_0 . In the same spirit, successive reversals of reference solenoid current were made while calibrating.

These observations were made at low as well as high rf intensity, so that full saturation curves were plotted out. Data fitting and extrapolation to "infinite" rf intensity will be discussed later. Figures 2 and 3 show typical data obtained for lithium and sodium at 1.5°K. The other saturation plots obtained at these and higher temperatures are of similar appearance.

Impurity Background

The shorted coaxial line containing the dispersions was constructed of nylon and gold foil, and at helium temperatures gave no detectable signal when empty. However, the lithium and sodium dispersions themselves contributed a small paramagnetic impurity resonance at helium temperatures. This background resonance was at roughly $g=2$, and was very broad in comparison to the metallic electron spin resonance. To

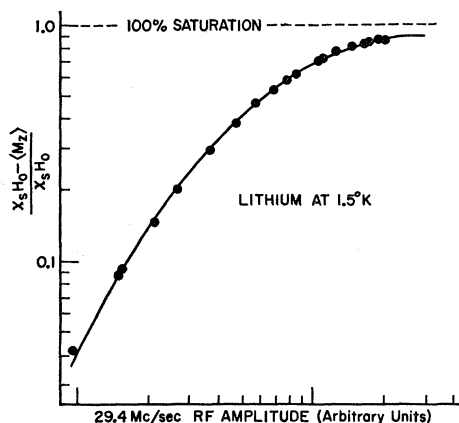


FIG. 2. The normalized steady-state change, at electron spin resonance, in the electron spin polarization of a $20\ \mu$ lithium dispersion at 1.5°K . A 29.4-Mc/sec transverse linearly polarized rf field is used. These data have been corrected for a paramagnetic impurity background signal of about 1%. The solid curve is derived from solutions to the modified Bloch equation and is chosen for best fit.

correct the data, additional saturation plots were taken well off the metallic resonance line center. From these plots, the background contribution to the total alternating sample moment was inferred. The uncertainty in this correction was about 2% of the metallic electron spin moment for the sodium data, and was negligible for the lithium data. It should be noted that the corrected data, shown in Figs. 2 and 3, are in good fit with the Overhauser enhancement data,¹⁰ which are unaffected by the impurity background.

Temperature Control

Since χ_s varies so little with temperature, precise thermometry was unnecessary, but care was taken to hold the sample temperature constant throughout a run. This was especially important for measurements on sodium, since T_1 in sodium is temperature-dependent while T_1 in lithium is not.

For ventilation, the dispersions were minced to a coarse powder, after first solidifying the oily dispersions by centrifuging. The coaxial line containing these powders had numerous slits. This arrangement proved adequate. At room temperature, the samples were barely warmed after several minutes exposure to saturation-level rf fields. At 77°K , the saturation plots obtained with different rf duty cycles for the same sodium sample were strictly proportional, indicating no change in T_1 . At 1.5°K , nuclear magnetic resonance measurements¹⁰ indicate that the particle temperature rises only to about 2°K when exposed to rf fields strong enough to saturate the electron spin resonance.

Rf Penetration

A test was made to verify that the rf field penetrates the lithium particles at low temperature. Lithium dis-

persion was packed into an rf coil; the inductance and Q of the coil at 28 Mc/sec were then measured at 300 , 77 , and 4.2°K . It is simple to prove that if the skin depth at low temperature still exceeds the particle diameter, then the fractional decrease in inductance, due to the increased exclusion of flux from the particles, just equals the increase in Q^{-1} , due to the increased eddy current dissipation in the particles. On the other hand, if the skin depth at low temperatures is much less than the particle diameter, the fractional decrease in inductance will be much larger than the change in Q^{-1} . After allowing for changes in the coil itself, it was found at 4.2°K that the changes in inductance and Q^{-1} were equal; at worst, the skin depth is not much smaller than the particle diameter. This test was not made on the sodium dispersions, which were too dilute to give adequate sensitivity. However, the sodium particles were only half the size of the lithium particles.

Dispersions

The samples for the room-temperature measurements of χ_s in lithium were obtained from two cans of the same 99.8% "low-sodium" grade dispersion previously used for measurements of nuclear T_1 in metals.¹¹ These samples proved to be better than any that could be made in the laboratory and, in fact, improved with age. After several years on the shelf, the electronic linewidth had decreased from about 1.5 to 0.8 G , possibly due to the precipitation of impurities. For the measurements of temperature dependence of χ_s in lithium, dispersion from the same cans was refined by thinning with mineral oil, separating the coarse particles by flotation, and then centrifuging the remaining suspension to a compact mass. Microscopic inspection showed

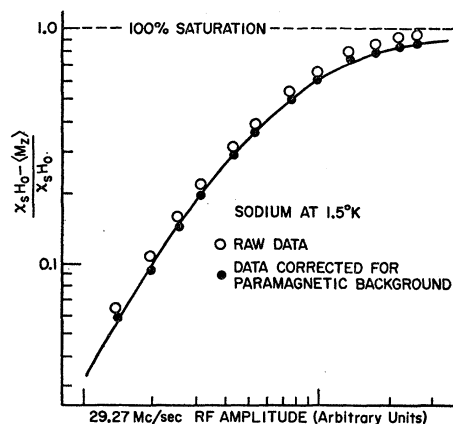


FIG. 3. The normalized steady-state change, at electron spin resonance, in the electron spin polarization of a $10\ \mu$ sodium dispersion at 1.5°K . A 29.27-Mc/sec transverse linearly polarized rf field is used. The dots are data corrected for paramagnetic impurity background; the circles are raw data. The solid curve is derived from solutions to the modified Bloch equation and is chosen for best fit.

¹¹ A. G. Anderson and A. G. Redfield, Phys. Rev. **116**, 583 (1959).

no particles greater than $20\ \mu$ in diameter in these refined samples.

For the measurements on sodium, a home-made dispersion of 99.9% purity sodium in ceresin wax was used. No particles greater than $10\ \mu$ in diameter were found. The linewidths in this dispersion were 2.8 G at 77 and 0.25 G at 1.5°K, about the same as those reported by Feher and Kip¹²; moreover, it was relatively free of paramagnetic impurities which, as noted earlier, contribute to the total alternating moment detected.

Chemical Analysis

The absolute measurements of χ_s in lithium were made at 300°K on corked vials of lithium dispersion, with a hairpin as an rf source. Corking was sufficient to protect the dispersion against atmospheric moisture for periods of weeks or months. After a series of runs on a given sample, the vial was broken into a flask through which a stream of purified oxygen flowed, and water was slowly dripped into the flask. The hydrogen evolved in the lithium-water reaction was carried by the oxygen stream through freeze-out traps and drying towers, and then to a hot platinum catalyzing chamber. The water produced here was trapped and weighed, and the original weight of lithium thus deduced. This chemical analysis was made and reported by Berkenblit and Reisman.¹³ A similar chemical analysis of sodium samples was not attempted, since several months effort, with a poor prospect of even 5% accuracy in χ_s , would have been required.

III. MODIFIED BLOCH EQUATION

Nature of Equation

The modified Bloch equation is the vector equation of motion for the magnetization of a system of nearly free spins in an applied magnetic field. For conduction electrons in a uniform field, the appropriate form of the equation has been shown to be⁸

$$\frac{d\mathbf{M}}{dt} = \gamma\mathbf{M} \times \mathbf{H} + \frac{\chi_s\mathbf{H} - \mathbf{M}}{T_1}, \quad (1)$$

where \mathbf{M} is the magnetization, \mathbf{H} is the instantaneous field, γ is the gyromagnetic ratio, χ_s is the spin susceptibility, and T_1 is the spin-lattice relaxation time, which equals the spin-spin relaxation time T_2 .

In the present experiment, \mathbf{H} is the vector sum of the polarizing field \mathbf{H}_0 and the transverse, linearly polarized rf field $2\mathbf{H}_1 \cos\omega t$. The relaxation time T_1 is roughly 10^{-7} sec, corresponding to a linewidth of roughly 1 G. Since H_0 is about 10 G, H_1 and H_0 are comparable at saturation. In this regard, the present experiment is atypical. The condition usually met is that $H_0 \gg H_1$, and the approximation can then be made that only a

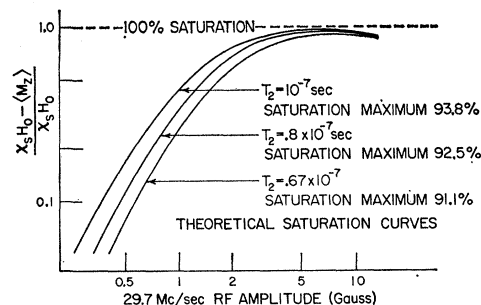


FIG. 4. The degree of saturation $Z = (\chi_s H_0 - \langle M_z \rangle) / \chi_s H_0$, for several values of T_1 , as a function of 29.7-Mc/sec transverse linearly polarized rf field strength at electron spin resonance. These curves are obtained by numerical integration of the modified Bloch equation.

single circularly polarized component of the rf field is effective. The counter-rotating component has been shown¹⁴ to produce a shift in the resonance by a relative amount $[H_1/2H_0]^2$, and also to produce weak resonances¹⁵ in polarizing fields which are odd multiples of ω/γ . Such effects can be expected to strongly modify the approach to saturation in this experiment; therefore, it was necessary that the modified Bloch equation be solved exactly.

Numerical Integration of the Modified Bloch Equation

A steady-state solution to the modified Bloch equation for which $\mathbf{H} = 2H_1 \cos(\omega t)\mathbf{i} + H_0\mathbf{k}$, was constructed as follows: Let

$$\mathbf{M}(t) = \mathbf{M}_0(t) + a\mathbf{M}_1(t) + b\mathbf{M}_2(t) + c\mathbf{M}_3(t), \quad (2)$$

where

$$\mathbf{M}_1(0) = \mathbf{i}, \quad \mathbf{M}_2(0) = \mathbf{j}, \quad \mathbf{M}_3(0) = \mathbf{k}, \quad \text{and} \quad \mathbf{M}_0(0) = 0.$$

In its evolution, let \mathbf{M}_0 obey the modified Bloch equation with χ_s equal to unity, and let \mathbf{M}_1 , \mathbf{M}_2 , and \mathbf{M}_3 obey the homogeneous equation $d\mathbf{M}/dt = \gamma\mathbf{M} \times \mathbf{H} - \mathbf{M}/T_1$. Since the steady motion is symmetric and surely repeats every cycle, the steady-state boundary condition at the end of a half-cycle is given by

$$\mathbf{M}(\pi/\omega) = -a\mathbf{i} - b\mathbf{j} + c\mathbf{k}. \quad (3)$$

The coefficients a , b , and c are then found by inverting Eq. (3), after individual numerical integrations to find $\mathbf{M}_0(\pi/\omega)$, $\mathbf{M}_1(\pi/\omega)$, $\mathbf{M}_2(\pi/\omega)$, and $\mathbf{M}_3(\pi/\omega)$. Individual averages of the z component are stored while generating these vectors, so that the time-average longitudinal magnetization $\langle M_z \rangle$ is found immediately from Eq. (2). Recalling that χ_s is unity here, the degree of saturation is then given by $Z = 1 - \langle M_z \rangle / H_0$.

Figure 4 shows a set of on-resonance saturation curves of Z against H_1 for several values of T_1 and a resonance frequency of 29.7 Mc/sec. It should be noted that the

¹² G. Feher and A. F. Kip, Phys. Rev. **98**, 337 (1955).

¹³ M. Berkenblit and A. Reisman, Anal. Chem. **32**, 721 (1960).

¹⁴ F. Bloch and A. Siegert, Phys. Rev. **57**, 522 (1940).

¹⁵ J. Winter, Compt. Rend. **241**, 375 (1955).

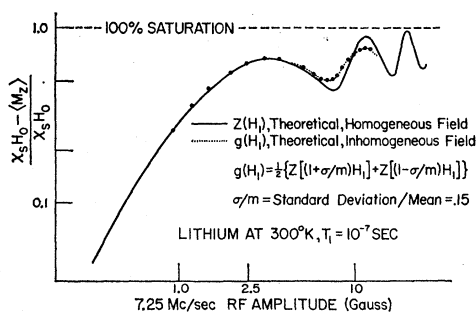


FIG. 5. The normalized steady-state change at electron spin resonance in the electron spin polarization of a $20\ \mu$ lithium dispersion at 300°K . A 7.25-Mc/sec transverse, linearly polarized rf field is used. The data depart from the computed solid curve because of rf inhomogeneity. The dotted curve is obtained by folding the solid curve on an rf field distribution whose ratio of standard deviation to mean is 0.15.

degree of saturation is not monotonic with increasing rf amplitude, but shows a peak. This behavior is more pronounced for on-resonance saturation at lower frequencies, as can be seen in Fig. 5. This theoretical result was tested by modifying the apparatus for observations at 7.25 Mc/sec. The experimental data depart from the solid computed curve because the applied rf field was not uniform over the sample volume. The dotted curve to which the data are fitted is a convolution of the solid curve with a distribution function chosen to give best fit, as will be described in Sec. IV.

To better understand these saturation peaks, the more tractable problem of square-wave (rather than sine-wave) rf excitation was solved analytically. The magnetization now precesses in a fixed cone (neglecting relaxation) about the resultant field direction for each half-cycle, the cone lying more and more horizontally with increasing rf amplitude. Because the motion is required to be re-entrant, the cone half-angle must alternately open and close with increasing rf amplitude, thus accounting for the peaks in Z . It was found that the higher order peaks are separated by intervals of rf amplitude equal to twice the polarizing field strength.

IV. DATA FITTING

Folded Saturation Curves

In the integration of the modified Bloch equation, a uniform rf field was assumed. Because the actual rf field varied throughout the sample cell, and more important, because rf penetration of the particles was incomplete at liquid-helium temperatures, the plots of signal against rf field strength show less curvature than the computed saturation curves. A source of further deviation, the possible existence of a distribution of relaxation times among the particles, was also considered. However, since the observed resonance lines did not appreciably depart from Lorentzian shape, it was concluded that such a distribution would have slight width and negligible effect on the experimental results.

At 300 and 77°K the skin depth exceeds the particle diameter, so that curves appropriate for data fitting could be generated by folding the computed saturation curves on the known rf field distribution. A graphical procedure was used which proved quite accurate. The rf field distribution was approximated by a pair of δ functions spaced one standard deviation σ to each side of the mean field m . For the shorted coaxial line, $\sigma = 0.16\ \text{m}$; for the rf hairpin, $\sigma = 0.15\ \text{m}$ (see Fig. 5). The sum of $\frac{1}{2}Z[(1+\sigma/m)H_1]$ and $\frac{1}{2}Z[(1-\sigma/m)H_1]$, obtained from the theoretical saturation curve for the appropriate T_1 and H_0 , was plotted against H_1 . Such folded curves were found to be practically indistinguishable from the exact convolutions of the rf field distribution with the saturation curve. In any event, these folded curves differ little from the original computed curves (except for an irrelevant change of H_1 scale) until σ becomes comparable with the width of a saturation peak.

Both the ordinate and abscissa scales of the folded saturation curve are adjusted to best fit the data, and the signal obtainable on full saturation is thereby deduced. This same graphical construction of folded saturation curves is used in fitting the data obtained at liquid-helium temperatures, where skin effect smearing predominates. A good apparent fit is obtained when the ratio σ/m is between 0.4 and 0.5, and the validity of this fit will be justified in the following section.

Correction for Skin Effect

The rf field only partially penetrates the particles at liquid-helium temperatures, and if it were true that for this reason some sample is "lost," the measurements of relative susceptibility would be worthless. We now show that incomplete rf penetration merely reduces the average rf field seen by the electrons, the reduction factor being roughly equal to the ratio of skin depth δ to particle radius r . The same result has been stated by Abragam.¹⁶ Our treatment is a modification of one first given by Dyson.¹⁷

An electron moves randomly inside a particle for a time $T_1 \approx 10^{-7}$ sec before making a spin-lattice collision. The diffusion length d during this time is given by $d = (v_F l T_1 / 3)^{1/2}$, where v_F is the Fermi velocity and l is the mean free path for ordinary collisions. At liquid-helium temperature, $l \geq 10^{-5}$ cm, so $d \geq 100\ \mu$, and the electron moves in and out of the particle skin many times before relaxing. Thus, every electron sees a statistically identical rf field whose amplitude fluctuates but whose phase is preserved. If the skin depth is much smaller than the radius, the electron sees the rf field in bursts of average duration T_δ separated by intervals of average duration T_r , where T_δ is the time spent in the skin and T_r is the time spent in the field-free interior.

¹⁶ A. Abragam, *Principles of Nuclear Magnetism* (Oxford University Press, London, 1961), p. 377.

¹⁷ F. J. Dyson, *Phys. Rev.* **98**, 349 (1955).

The power spectrum of such a waveform can be derived from its autocorrelation function by applying the Wiener-Khinchin relation. The power spectrum will be a δ function centered at the applied radio frequency, superimposed on a broad weak base whose width is of order T_δ^{-1} or T_r^{-1} , depending on the degree of correlation between bursts. The important result is that the δ function has an intensity corresponding to an uninterrupted uniform rf field of amplitude $2H_1T_\delta/T_r$. The signal observed at resonance will then be the same as for a particle uniformly penetrated by an uninterrupted rf field of amplitude $2H_1T_\delta/T_r$, or roughly $2H_1\delta/r$. The same result could be derived by considering the spin in a rotating reference frame, precessing stepwise around the fixed effective field direction. At resonance, the average precession rate around H_1 is reduced by a factor T_δ/T_r .

Thus, incomplete rf penetration in a dispersion of uniform particle size should affect only the H_1 scale, but not the shape of the saturation curve. However, a distribution of particle size will tend to smear the curve shape, but as found by the analysis sketched below, this smearing is well approximated by curves folded in the manner described in the preceding section.

The approximation was first made that particles for which $r \geq \delta$ experience a reduced rf field $(\delta/r)2H_1 \cos \omega t$, while smaller particles experience the full applied rf field. Analysis then showed that for any reasonably smooth particle size distribution, the ratio σ/m for the resulting effective rf field distribution would rapidly approach a value $\sigma/m = (\langle r \rangle \langle r^3 \rangle - \langle r^2 \rangle^2)^{1/2} / \langle r \rangle^2$ in the limit $\langle r \rangle \gg \delta$. The data obtained at liquid-helium temperature were in good apparent fit with folded curves for which σ/m was about 0.4 or 0.5, and for which m was about 40% of the mean applied rf field. Two trial particle size distributions were then considered. These were of the form $\exp(-x^2)$ and $x^2 \exp(-x)$, ($x \propto r/\delta$), and when scaled so that $\delta = 0.82\langle r \rangle$ and $\delta = 0.68\langle r \rangle$ respectively, generated effective rf field distributions for which $m = 0.4$ for each, and $\sigma/m = 0.49$ and $\sigma/m = 0.45$, respectively. These rf field distributions were then machine convoluted with a theoretical saturation curve, and each convolution was compared with the curve obtained, as described in the previous section, by simply folding the saturation curve on σ/m . The machine convoluted curves both agreed with the folded curves to about 1%. Finally, it was observed that there

TABLE I. Conduction electron spin susceptibility in lithium.

Sample	Mass ^a (g)	$\chi_s \times 10^6$ (cgs volume units)
L. S. 9	0.819	1.97
L. S. 11	0.648	1.99
L. S. 12	0.710	1.95
L. S. 13	0.865	1.90
L. S. 14	0.739	1.97

^a See Ref. 13.

TABLE II. Theoretical and experimental values of χ_s for lithium and sodium, in cgs volume units $\times 10^6$.

Lithium	Sodium	Method
1.17	0.64	Free-electron model ^a
5.3	1.7	Free-electron model, with exchange and correlation corrections. ^b
1.87	0.85	Collective coordinate model. ^c
2.12	0.967	Collective coordinate model. ^d
2.08 ± 0.10	0.95 ± 0.10	Comparison of ESR with NMR. ^e
	1.13 ± 0.10	Comparison of ESR with NMR. ^f
1.98 ± 0.10		Measurement of P_F , ^g combined with
1.90 ± 0.10		measurement of Knight shift. ^{h,i}
1.96 ± 0.10		Present measurement (ESR saturation)

^a See Ref. 3.

^b J. B. Sampson and F. Seitz, Phys. Rev. **56**, 633 (1940).

^c See Ref. 4.

^d See Ref. 5.

^e See Ref. 1.

^f See Ref. 2.

^g Ch. Rytter, Phys. Rev. Letters **5**, 10 (1960). Rytter's value of $\xi = 0.442 \pm 0.015$ is here corrected to $\xi = 0.475 \pm 0.020$, in view of our result (see Ref. 10) that the saturated Overhauser enhancement in lithium is 0.93 (γ_e/γ_n). This corrected value of ξ is then combined with the reported Knight shifts in lithium (See footnotes h and i) to yield the tabulated values of χ_s . Knight (Ref. 6) suggests that a chemical shift may be the cause of the discrepancy in these reported shifts, as different reference lithium compounds were used.

^h H. S. Gutowsky and B. R. McGarvey, J. Chem. Phys. **20**, 1472 (1952).

ⁱ D. F. Abell and W. D. Knight (unpublished), but see Ref. 6, Table IV.

was less than 1% difference between the electron spin moments inferred by fitting the data to curves folded on $\sigma/m = 0.4$ and $\sigma/m = 0.5$. It was concluded that a good fit to a folded saturation curve was a sufficient criterion for valid inference of the electron spin moment, whatever the particle size distribution, provided only that no large particles were present. Absence of large particles is almost certain, as evidenced by microscopic examination, by the equality of the change in sample Q^{-1} to the change in sample inductance, and by the similarity of the saturation curves obtained at 300°K to those obtained at 77°K. As further evidence, in the experiment described in the paper immediately following,¹⁰ full Overhauser enhancement was obtained at a nuclear spin resonance frequency of about 1.16 Mc/sec while the electron spin resonance frequency was at 29 Mc/sec.

V. RESULTS

Table I gives values of χ_s for five samples of lithium; the average value is $\chi_s = (1.96 \pm 0.10) \times 10^{-6}$ cgs volume units. Table II compares this result with other reported values of χ_s . It is also possible to derive a value of χ_s from the Korringa relation, as will be discussed in the paper immediately following.¹⁰ However, such a value is apt to be in error because of the uncertainty in electronic specific heat. Reported values for the electronic specific heat in lithium^{18,19} and in sodium¹⁹⁻²¹ differ

¹⁸ L. M. Roberts, *Low Temperature Physics and Chemistry*, edited by J. R. Dillinger (University of Wisconsin Press, Madison, 1958), p. 417.

¹⁹ D. L. Martin, Proc. Roy. Soc. (London) **A263**, 378 (1961).

²⁰ R. E. Gaumer and C. V. Heer, Phys. Rev. **118**, 955 (1960).

²¹ W. H. Lien and N. E. Phillips, Phys. Rev. **118**, 958 (1960).

among themselves, and more important, were obtained with bulk samples which are known to undergo a partial martensitic transformation²² at low temperatures. This transformation is probably inhibited in dispersed samples.²³ Despite these uncertainties, when measured values of the Knight shift,⁶ the nuclear spin-lattice relaxation time,^{10,11} and the average of the reported values of electronic specific heat are combined, one infers from the Korringa relation a value $\chi_s = (2.30 \pm 0.20) \times 10^{-6}$ cgs volume units for lithium, and $\chi_s = (1.06 \pm 0.10) \times 10^{-6}$ cgs volume units for sodium, in good agreement with the values given in Table II.

The relative values of χ_s in lithium were the same at 300, 77, and 1.5°K, within an estimated uncertainty of 3%, and were the same in sodium at 77 and 1.5°K, within an estimated uncertainty of 5%. This result for sodium is in agreement with that reported by Schu-

macher and Vehse.² Feldman and Knight²⁴ have reported an anomalously large decrease of the Knight shift in sodium at low temperature, which could be accounted for by about a 2% decrease of χ_s in sodium at 4.2°K, or conversely, by an additional 2% decrease in P_F over its estimated decrease. Unfortunately, neither the measurements of Schumacher and Vehse nor our measurements are sufficiently precise to resolve this uncertainty.

ACKNOWLEDGMENTS

The author wishes to express his thanks to Dr. A. G. Redfield for having suggested this research and for his continued encouragement and support, to Dr. R. L. Garwin for many stimulating and informative discussions, and to R. J. Blume and W. V. Kiselewsky for their valuable technical advice and assistance.

²² C. S. Barrett, *Acta Cryst.* **9**, 671 (1956).

²³ Douglas L. Martin (private communication).

²⁴ D. W. Feldman, thesis, University of California, 1960 (unpublished).

Overhauser Effect in Metallic Lithium and Sodium*

RICHARD HECHT†

AND

ALFRED G. REDFIELD

IBM Watson Laboratory, Columbia University, New York, New York

(Received 12 June 1963)

The Overhauser polarization of nuclear spins in Li and Na metal has been precisely measured at 1.5°K and 10.4 G. The electron spin resonance was saturated for a time long compared to the nuclear spin relaxation time, and the resulting Overhauser polarization was then measured by adiabatically applying a high field and sweeping through nuclear resonance in a time short compared to the nuclear relaxation time. The degree of electron saturation was determined with precision by comparison with the change in electron spin magnetization longitudinally measured under the same experimental conditions. For Na the polarization ratio is $100 \pm 3\%$ of its high-field theoretical value γ_e/γ_n ; for Li, $84 \pm 3\%$. At 10.4 G correction must be made for polarization leakage via the nuclear spin-spin energy; the predicted ratios are 98.5% for Na and 90% for Li, of the high-field values. The remaining discrepancy in Li is presumably a result of conduction electron orbital contribution to the relaxation which is important because of the predominantly *p* character of the lithium conduction electron wave functions. The orbital relaxation rate is estimated theoretically for Li, and the result agrees with experiment.

INTRODUCTION

THAT the nuclear spin polarization in a metal would become greatly enhanced if the conduction electron spin resonance were saturated has been shown by Overhauser.¹ Of the several methods^{2,3} of dynamic nuclear polarization, the Overhauser effect is the one

which goes most strongly against intuition, so that its experimental observation by Carver and Slichter⁴ was of considerable interest. Overhauser predicted that the maximum enhancement of the nuclear spin polarization would be γ_e/γ_n times its thermal equilibrium value, where γ_e and γ_n are the electronic and nuclear gyromagnetic ratios. Quantitative confirmation of this prediction in Li can be inferred indirectly from measurement of the Overhauser-enhanced electronic Knight shift, the electronic spin susceptibility, and the nuclear Knight shift.⁵ It is directly confirmed with precision

* Part of this work was submitted by one of us (R. Hecht) in partial fulfillment of the requirements for the degree of Doctor of Philosophy at Columbia University.

† Present address: R. C. A. Laboratories, Princeton, New Jersey.

¹ A. W. Overhauser, *Phys. Rev.* **92**, 411 (1953).

² A. Kastler, *J. Phys. Radium* **11**, 255 (1950).

³ R. V. Pound, *J. Phys. Chem.* **57**, 743 (1953).

⁴ T. R. Carver and C. P. Slichter, *Phys. Rev.* **102**, 975 (1956).

⁵ Ch. Rytter, *Phys. Rev. Letters* **5**, 10 (1960).